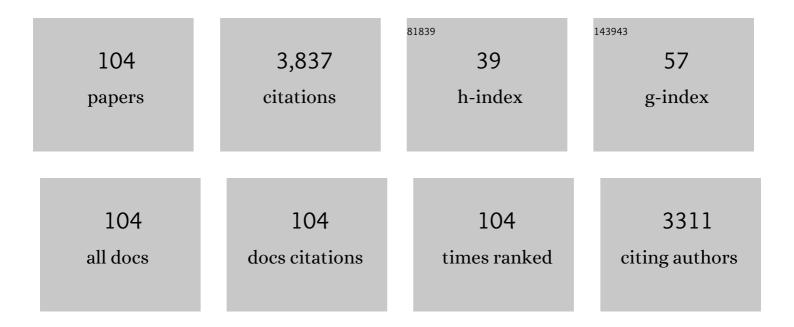
## Xidong Wang

List of Publications by Year in descending order

Source: https://exaly.com/author-pdf/11041717/publications.pdf Version: 2024-02-01



#	Article	IF	CITATIONS
1	ANN-based structure-viscosity relationship model of multicomponent slags for production design in mineral wool. Construction and Building Materials, 2022, 319, 126010.	3.2	12
2	Investigation of cooling processes of molten slags to develop multilevel control method for cleaner production in mineral wool. Journal of Cleaner Production, 2022, 339, 130548.	4.6	7
3	Ultralow loading of Cu2O/CuO nanoparticles on metal-organic framework-derived carbon octahedra and activated semi-coke for highly efficient SO2 removal. Journal of Cleaner Production, 2022, 341, 130823.	4.6	17
4	Experimental Investigation of Vitrification Process for the Disposal of Hazardous Solid Waste Containing Chlorides. Processes, 2022, 10, 526.	1.3	0
5	Designing Structure–Thermodynamics-Informed Artificial Neural Networks for Surface Tension Prediction of Multi-component Molten Slags. Metallurgical and Materials Transactions B: Process Metallurgy and Materials Processing Science, 2022, 53, 2018-2029.	1.0	4
6	Mechanistic and Experimental Study of the CuxO@C Nanocomposite Derived from Cu3(BTC)2 for SO2 Removal. Catalysts, 2022, 12, 689.	1.6	0
7	Computational Screening and Synthesis of M (M = Mo and Cu)-Doped CeO <sub>2</sub> /silicalite-1 for Medium-/Low-Temperature NH <sub>3</sub> –SCR. Industrial & Engineering Chemistry Research, 2022, 61, 10091-10105.	1.8	8
8	Preparation, Sintering Behavior and Consolidation Mechanism of Vanadium-Titanium Magnetite Pellets. Crystals, 2021, 11, 188.	1.0	11
9	Three-Stage Method Energy–Mass Coupling High-Efficiency Utilization Process of High-Temperature Molten Steel Slag. Metallurgical and Materials Transactions B: Process Metallurgy and Materials Processing Science, 2021, 52, 3004-3015.	1.0	7
10	Structural and Viscous Insight into Impact of MoO3 on Molten Slags. Metallurgical and Materials Transactions B: Process Metallurgy and Materials Processing Science, 2021, 52, 3730-3743.	1.0	11
11	Development of structure-informed artificial neural network for accurately modeling viscosity of multicomponent molten slags. Ceramics International, 2021, 47, 30691-30701.	2.3	16
12	Promoting Effect of Ti Species in MnOx-FeOx/Silicalite-1 for the Low-Temperature NH3-SCR Reaction. Catalysts, 2020, 10, 566.	1.6	8
13	Highly dispersed MnO <sub>x</sub> –FeO <sub>x</sub> supported by silicalite-1 for the selective catalytic reduction of NO <sub>x</sub> with NH <sub>3</sub> at low temperatures. Catalysis Science and Technology, 2020, 10, 5525-5534.	2.1	6
14	In Situ DRIFTS Investigation on CeOx Catalyst Supported by Fly-Ash-Made Porous Cordierite Ceramics for Low-Temperature NH3-SCR of NOX. Catalysts, 2019, 9, 496.	1.6	10
15	Insight into the Relationship Between Viscosity and Structure of CaO-SiO2-MgO-Al2O3 Molten Slags. Metallurgical and Materials Transactions B: Process Metallurgy and Materials Processing Science, 2019, 50, 2930-2941.	1.0	57
16	Manganese oxide catalysts supported on zinc oxide nanorod arrays: A new composite for selective catalytic reduction of NOx with NH3 at low temperature. Applied Surface Science, 2019, 491, 579-589.	3.1	25
17	Kinetic studies on bituminous coal char gasification using CO <sub>2</sub> and H <sub>2</sub> O mixtures. International Journal of Green Energy, 2019, 16, 1144-1151.	2.1	11
18	Fabrication and characterization of porous cordierite ceramics prepared from fly ash and natural minerals. Ceramics International, 2019, 45, 18306-18314.	2.3	40

#	Article	IF	CITATIONS
19	Reuse of mineral wool waste and recycled glass in ceramic foams. Ceramics International, 2019, 45, 15057-15064.	2.3	55
20	Synthesis of a foam ceramic based on ceramic tile polishing waste using SiC as foaming agent. Ceramics International, 2018, 44, 10078-10086.	2.3	62
21	Application of washed MSWI fly ash in cement composites: long-term environmental impacts. Environmental Science and Pollution Research, 2018, 25, 12127-12138.	2.7	29
22	Recycling of municipal solid waste incineration by-product for cement composites preparation. Construction and Building Materials, 2018, 162, 794-801.	3.2	84
23	Integrated utilization of fly ash and waste glass for synthesis of foam/dense bi-layered insulation ceramic tile. Energy and Buildings, 2018, 168, 67-75.	3.1	32
24	Roles of P <sub>2</sub> O <sub>5</sub> Addition on the Viscosity and Structure of CaO–SiO <sub>2</sub> –Al <sub>2</sub> O <sub>3</sub> –Na <sub>2 Melts. ISIJ International, 2018, 58, 1644-1649.</sub>	&l <b>tp/s</b> ub&	gt; <b>Dâ</b> €"P<s
25	Recycling ground MSWI bottom ash in cement composites: Long-term environmental impacts. Waste Management, 2018, 78, 841-848.	3.7	46
26	Integrated utilization of high alumina fly ash for synthesis of foam glass ceramic. Ceramics International, 2018, 44, 13681-13688.	2.3	55
27	Long-term leaching behaviours of cement composites prepared by hazardous wastes. RSC Advances, 2018, 8, 27602-27609.	1.7	5
28	Solid wastes utilization in the iron and steel industry in China: towards sustainability. Institutions of Mining and Metallurgy Transactions Section C: Mineral Processing and Extractive Metallurgy, 2017, 126, 41-46.	0.6	8
29	Preparation and characterization of permeable bricks from gangue and tailings. Construction and Building Materials, 2017, 148, 484-491.	3.2	47
30	Preparation and characterization of the one-piece wall ceramic board by using solid wastes. Ceramics International, 2017, 43, 8564-8571.	2.3	14
31	Synthesis of a ceramic tile base based on high-alumina fly ash. Construction and Building Materials, 2017, 155, 930-938.	3.2	42
32	Promotional effect of rare earth-doped manganese oxides supported on activated semi-coke for selective catalytic reduction of NO with NH3. Environmental Science and Pollution Research, 2017, 24, 24473-24484.	2.7	23
33	Effect of water-washing on the co-removal of chlorine and heavy metals in air pollution control residue from MSW incineration. Waste Management, 2017, 68, 221-231.	3.7	62
34	Role of steel slags on biomass/carbon dioxide gasification integrated with recovery of high temperature heat. Bioresource Technology, 2017, 223, 1-9.	4.8	21
35	Integrated Utilization of Sewage Sludge and Coal Gangue for Cement Clinker Products: Promoting Tricalcium Silicate Formation and Trace Elements Immobilization. Materials, 2016, 9, 275.	1.3	17
36	Integrated biomass gasification using the waste heat from hot slags: Control of syngas and polluting gas releases. Energy, 2016, 114, 165-176.	4.5	17

#	Article	IF	CITATIONS
37	A Fe-C-Ca big cycle in modern carbon-intensive industries: toward emission reduction and resource utilization. Scientific Reports, 2016, 6, 22323.	1.6	6
38	Integration of biomass/steam gasification with heat recovery from hot slags: Thermodynamic characteristics. International Journal of Hydrogen Energy, 2016, 41, 5916-5926.	3.8	24
39	Effect of Al2O3 Addition on the Precipitated Phase Transformation in Ti-Bearing Blast Furnace Slags. Metallurgical and Materials Transactions B: Process Metallurgy and Materials Processing Science, 2016, 47, 1390-1399.	1.0	21
40	In situ DRIFTS studies on MnO nanowires supported by activated semi-coke for low temperature selective catalytic reduction of NO with NH3. Applied Surface Science, 2016, 366, 139-147.	3.1	71
41	Environmental investigation on co-combustion of sewage sludge and coal gangue: SO 2 , NO x and trace elements emissions. Waste Management, 2016, 50, 213-221.	3.7	108
42	Integration of coal gasification and waste heat recovery from high temperature steel slags: an emerging strategy to emission reduction. Scientific Reports, 2015, 5, 16591.	1.6	19
43	Facile and Economical Preparation of SiAlON-Based Composites Using Coal Gangue: From Fundamental to Industrial Application. Energies, 2015, 8, 7428-7440.	1.6	9
44	Co-modification and Crystalline-control of Ti-bearing Blast Furnace Slags. ISIJ International, 2015, 55, 158-165.	0.6	25
45	Preparation and modeling of energy-saving building materials by using industrial solid waste. Energy and Buildings, 2015, 97, 6-12.	3.1	10
46	Integrated carbon dioxide/sludge gasification using waste heat from hot slags: Syngas production and sulfur dioxide fixation. Bioresource Technology, 2015, 181, 174-182.	4.8	53
47	Investigation on slag fiber characteristics: Mechanical property and anti-corrosion performance. Ceramics International, 2015, 41, 5677-5687.	2.3	20
48	Promoting effect of Nd on the reduction of NO with NH <sub>3</sub> over CeO <sub>2</sub> supported by activated semi-coke: an in situ DRIFTS study. Catalysis Science and Technology, 2015, 5, 2251-2259.	2.1	105
49	A Novel Kinematic Model for Molten Slag Fiberization: Prediction of Slag Fiber Properties. Metallurgical and Materials Transactions B: Process Metallurgy and Materials Processing Science, 2015, 46, 993-1001.	1.0	12
50	Achieving waste to energy through sewage sludge gasification using hot slags: syngas production. Scientific Reports, 2015, 5, 11436.	1.6	27
51	Heat Recovery from High Temperature Slags: A Review of Chemical Methods. Energies, 2015, 8, 1917-1935.	1.6	83
52	Synthesis, characterization and modeling of new building insulation material using ceramic polishing waste residue. Construction and Building Materials, 2015, 85, 119-126.	3.2	63
53	Fuel nitrogen conversion and release of nitrogen oxides during coal gangue calcination. Environmental Science and Pollution Research, 2015, 22, 7139-7146.	2.7	23
54	FTIR, Raman and NMR investigation of CaO–SiO2–P2O5 and CaO–SiO2–TiO2–P2O5 glasses. Journal o Non-Crystalline Solids, 2015, 420, 26-33.	of 1.5	102

#	Article	IF	CITATIONS
55	Facile and economical synthesis of porous activated semi-cokes for highly efficient and fast removal of microcystin-LR. Journal of Hazardous Materials, 2015, 299, 325-332.	6.5	17
56	Trace element partitioning behavior of coal gangue-fired CFB plant: experimental and equilibrium calculation. Environmental Science and Pollution Research, 2015, 22, 15469-15478.	2.7	29
57	Two-stage high temperature sludge gasification using the waste heat from hot blast furnace slags. Bioresource Technology, 2015, 198, 364-371.	4.8	45
58	Thermodynamic modeling of electrolyte solutions by a hybrid ion-interaction and solvation (HIS) model. Calphad: Computer Coupling of Phase Diagrams and Thermochemistry, 2015, 48, 79-88.	0.7	5
59	Effects of chemistry and mineral on structural evolution and chemical reactivity of coal gangue during calcination: towards efficient utilization. Materials and Structures/Materiaux Et Constructions, 2015, 48, 2779-2793.	1.3	48
60	Effect of P2O5 Addition on the Viscosity and Structure of Titanium Bearing Blast Furnace Slags. ISIJ International, 2014, 54, 1491-1497.	0.6	23
61	Effect of B2O3 on the Structure and Viscous Behavior of Ti-Bearing Blast Furnace Slags. Jom, 2014, 66, 2168-2175.	0.9	55
62	Multi-Stage Control of Waste Heat Recovery from High Temperature Slags Based on Time Temperature Transformation Curves. Energies, 2014, 7, 1673-1684.	1.6	42
63	Preparation of Slag Wool by Integrated Waste-Heat Recovery and Resource Recycling of Molten Blast Furnace Slags: From Fundamental to Industrial Application. Energies, 2014, 7, 3121-3135.	1.6	40
64	Characteristics of low temperature biomass gasification and syngas release behavior using hot slag. RSC Advances, 2014, 4, 62105-62114.	1.7	36
65	Numerical modeling and experimental study of heat transfer in ceramic fiberboard. Textile Reseach Journal, 2014, 84, 411-421.	1.1	16
66	Pyrite transformation and sulfur dioxide release during calcination of coal gangue. RSC Advances, 2014, 4, 42506-42513.	1.7	27
67	Experimental investigation and modeling of cooling processes of high temperature slags. Energy, 2014, 76, 761-767.	4.5	61
68	Development of the random simulation model for estimating the effective thermal conductivity of insulation materials. Building and Environment, 2014, 80, 221-227.	3.0	21
69	In situ DRIFTS investigation on the SCR of NO with NH3 over V2O5 catalyst supported by activated semi-coke. Applied Surface Science, 2014, 313, 660-669.	3.1	145
70	Investigation of the Viscosity and Structural Properties of CaO-SiO2-TiO2 Slags. Metallurgical and Materials Transactions B: Process Metallurgy and Materials Processing Science, 2014, 45, 1389-1397.	1.0	99
71	The Effect of P2O5 on the Crystallization Behaviors of Ti-Bearing Blast Furnace Slags Using Single Hot Thermocouple Technique. Metallurgical and Materials Transactions B: Process Metallurgy and Materials Processing Science, 2014, 45, 1446-1455.	1.0	40
72	Low-temperature SCR of NO with NH3 over activated semi-coke composite-supported rare earth oxides. Applied Surface Science, 2014, 309, 1-10.	3.1	71

#	Article	IF	CITATIONS
73	Tailoring CoO–ZnO nanorod and nanotube arrays for Li-ion battery anode materials. Journal of Materials Chemistry A, 2013, 1, 9654.	5.2	59
74	Raman spectroscopic study of the structural properties of CaO–MgO–SiO2–TiO2 slags. Journal of Non-Crystalline Solids, 2013, 376, 209-215.	1.5	79
75	Activated Semi-coke in SO <sub>2</sub> Removal from Flue Gas: Selection of Activation Methodology and Desulfurization Mechanism Study. Energy & Fuels, 2013, 27, 3080-3089.	2.5	78
76	Influence of Basicity and TiO2 Content on the Precipitation Behavior of the Ti-bearing Blast Furnace Slags. ISIJ International, 2013, 53, 1696-1703.	0.6	50
77	Hydrothermal Synthesis of CeO <sub>2</sub> Nanoparticles on Activated Carbon with Enhanced Desulfurization Activity. Energy & Fuels, 2012, 26, 5879-5886.	2.5	45
78	Effect of Substrate Pretreatment on Controllable Growth of TiO2 Nanorod Arrays. Journal of Materials Science and Technology, 2012, 28, 577-586.	5.6	20
79	Ultrasensitive sorption behavior of isostructural lanthanide–organic frameworks induced by lanthanide contraction. Journal of Materials Chemistry, 2012, 22, 21076.	6.7	48
80	Conductivity properties of Î <sup>2</sup> -SiAlON ceramics. Science China Technological Sciences, 2012, 55, 2409-2415.	2.0	7
81	Pore size-controlled gases and alcohols separation within ultramicroporous homochiral lanthanide–organic frameworks. Journal of Materials Chemistry, 2012, 22, 7813.	6.7	53
82	Effect of Al <sub>2</sub> O <sub>3</sub> /SiO <sub>2</sub> Ratio on the Viscosity and Structure of Slags. ISIJ International, 2012, 52, 753-758.	0.6	90
83	Crystallization Behavior of Rutile in the Synthesized Ti-bearing Blast Furnace Slag Using Single Hot Thermocouple Technique. ISIJ International, 2011, 51, 1396-1402.	0.6	58
84	The Influence of SiO <sub>2</sub> on the Extraction of Ti Element from Tiâ€bearing Blast Furnace Slag. Steel Research International, 2011, 82, 607-614.	1.0	55
85	Electrochemical deposition of branched hierarchical ZnO nanowire arrays and its photoelectrochemical properties. Electrochimica Acta, 2011, 56, 5776-5782.	2.6	68
86	Hydrothermal growth of well-aligned TiO2 nanorod arrays: Dependence of morphology upon hydrothermal reaction conditions. Rare Metals, 2010, 29, 286-291.	3.6	40
87	Hydrothermal synthesis and characterization of TiO2 nanorod arrays on glass substrates. Materials Research Bulletin, 2009, 44, 1232-1237.	2.7	98
88	Calculations of Freezing Point Depression, Boiling Point Elevation, Vapor Pressure and Enthalpies ofÂVaporization of Electrolyte Solutions by a Modified Three-Characteristic Parameter Correlation Model. Journal of Solution Chemistry, 2009, 38, 1097-1117.	0.6	22
89	Thermodynamic study and syntheses of Î <sup>2</sup> -SiAlON ceramics. Science in China Series D: Earth Sciences, 2009, 52, 3122-3127.	0.9	9
90	Estimation of Freezing Point Depression, Boiling Point Elevation, and Vaporization Enthalpies of Electrolyte Solutions. Industrial & Engineering Chemistry Research, 2009, 48, 2229-2235.	1.8	34

#	Article	IF	CITATIONS
91	A Simple Two-Parameter Correlation Model for Aqueous Electrolyte Solutions across a Wide Range of Temperatures. Journal of Chemical & Engineering Data, 2009, 54, 179-186.	1.0	17
92	Effects of preparing conditions on the electrodeposition of well-aligned ZnO nanorod arrays. Electrochimica Acta, 2008, 53, 4633-4641.	2.6	62
93	Correlation and Prediction of Thermodynamic Properties of Nonaqueous Electrolytes by the Modified TCPC Model. Journal of Chemical & Engineering Data, 2008, 53, 149-159.	1.0	16
94	Correlation and Prediction of Thermodynamic Properties of Some Complex Aqueous Electrolytes by the Modified Three-Characteristic-Parameter Correlation Model. Journal of Chemical & Engineering Data, 2008, 53, 950-958.	1.0	22
95	Correlation and Prediction of Activity and Osmotic Coefficients of Aqueous Electrolytes at 298.15 K by the Modified TCPC Model. Journal of Chemical & Engineering Data, 2007, 52, 538-547.	1.0	43
96	Density-controlled hydrothermal growth of well-aligned ZnO nanorod arrays. Nanotechnology, 2007, 18, 035605.	1.3	169
97	A new three-particle-interaction model to predict the thermodynamic properties of different electrolytes. Journal of Chemical Thermodynamics, 2007, 39, 602-612.	1.0	11
98	Synthesis, evaluation and characterization of alumina ceramics with elongated grains. Ceramics International, 2005, 31, 953-958.	2.3	28
99	Kinetic studies of oxidation of γ-AlON–TiN composites. Journal of Alloys and Compounds, 2005, 387, 74-81.	2.8	12
100	Slag corrosion of gamma aluminium oxynitride. Steel Research = Archiv Für Das Eisenhüttenwesen, 2002, 73, 91-96.	0.2	3
101	Estimation of viscosity of ternary-metallic melts. Metallurgical and Materials Transactions A: Physical Metallurgy and Materials Science, 2002, 33, 3201-3204.	1.1	16
102	Kinetic studies of the oxidation of γ-aluminum oxynitride. Metallurgical and Materials Transactions B: Process Metallurgy and Materials Processing Science, 2002, 33, 201-207.	1.0	16
103	Thermodynamic study and synthesis of gamma-aluminum oxynitride. Scandinavian Journal of Metallurgy, 2002, 31, 1-6.	0.3	23
104	Preparation and Numerical Modelling of Ceramic Foam Insulation for Energy Saving in Buildings. , 0, , .		0